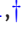RESEARCH ARTICLE

Inactivation of TRPM7 Kinase Targets AKT Signaling and Cyclooxygenase-2 Expression in Human CML Cells

Birgit Hoeger [1,†], Wiebke Nadolni[2,†], Sarah Hampe[2], Kilian Hoelting[2], Marco Fraticelli[2], Nadja Zaborsky[3,4,5], Anna Madlmayr[1], Viktoria Sperrer[1], Laura Fraticelli[2], Lynda Addington[2], Dirk Steinritz[2], Vladimir Chubanov[2], Roland Geisberger [3,4,5], Richard Greil[3,4,5], Andreas Breit[2], Ingrid Boekhoff[2], Thomas Gudermann[2], Susanna Zierler [1,2,*]

[1]Institute of Pharmacology, Johannes Kepler University Linz, Altenbergerstr. 69, 4040 Linz and Krankenhausstr. 5, 4020 Linz, Austria, [2]Walther Straub Institute of Pharmacology and Toxicology, Faculty of Medicine, Ludwig-Maximilians-Universität München, Goethestr. 33, 80336 Munich, Germany, [3]Department of Internal Medicine III with Haematology, Medical Oncology, Haemostaseology, Infectiology and Rheumatology, Oncologic Center, Paracelsus Medical University, 5020 Salzburg, Austria, [4]Salzburg Cancer Research Institute–Laboratory for Immunological and Molecular Cancer Research (SCRI–LIMCR), Müllner Hauptstr. 48, 5020 Salzburg, Austria and [5]Cancer Cluster Salzburg, 5020 Salzburg, Austria

*Address correspondence to S.Z. (e-mail: susanna.zierler@jku.at)

†Birgit Hoeger and Wiebke Nadolni contributed equally to this work.

Abstract

Cyclooxygenase-2 (COX-2) is a key regulator of inflammation. High constitutive *COX-2* expression enhances survival and proliferation of cancer cells, and adversely impacts antitumor immunity. The expression of *COX-2* is modulated by various signaling pathways. Recently, we identified the melastatin-like transient-receptor-potential-7 (TRPM7) channel-kinase as modulator of immune homeostasis. TRPM7 protein is essential for leukocyte proliferation and differentiation, and upregulated in several cancers. It comprises of a cation channel and an atypical α-kinase, linked to inflammatory cell signals and associated with hallmarks of tumor progression. A role in leukemia has not been established, and signaling pathways are yet to be deciphered. We show that inhibiting TRPM7 channel-kinase in chronic myeloid leukemia (CML) cells results in reduced constitutive *COX-2* expression. By utilizing a CML-derived cell line, HAP1, harboring CRISPR/Cas9-mediated TRPM7 knockout, or a point mutation inactivating TRPM7 kinase, we could link this to reduced activation of AKT serine/threonine kinase and mothers against decapentaplegic homolog 2 (SMAD2). We identified AKT as a direct in vitro substrate of TRPM7 kinase. Pharmacologic blockade of TRPM7 in wildtype HAP1 cells confirmed the effect on

COX-2 via altered AKT signaling. Addition of an AKT activator on TRPM7 kinase-dead cells reconstituted the wildtype phenotype. Inhibition of TRPM7 resulted in reduced phosphorylation of AKT and diminished *COX-2* expression in peripheral blood mononuclear cells derived from CML patients, and reduced proliferation in patient-derived CD34$^+$ cells. These results highlight a role of TRPM7 kinase in AKT-driven *COX-2* expression and suggest a beneficial potential of TRPM7 blockade in COX-2-related inflammation and malignancy.
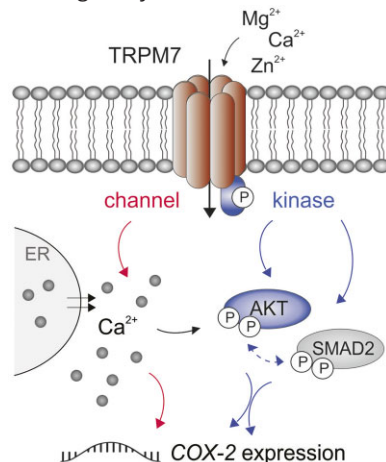
Key words: TRPM7; channel-kinase; CML; AKT signaling; COX-2

Introduction

The ubiquitously expressed melastatin-like transient-receptor-potential-7 (TRPM7) cation channel regulates immune system homeostasis, inflammation, and malignant progression.[1–11] TRPM7 primarily localizes to the plasma membrane and consists of a channel pore conducting divalent cations (Mg^{2+}, Ca^{2+}, Zn^{2+}), fused to an intracellular and constitutively active C-terminal serine/threonine α-kinase, which may convey separate signaling capacity.[12–14] TRPM7 channel and kinase are interdependent in that Mg^{2+} enters through the channel, and the kinase domain requires Mg^{2+} to function. The TRPM7 protein is essential for embryonic development and thymopoiesis.[15] TRPM7 kinase-inactivated mice are viable but show defects in T-cell, pancreatic beta-cell, and platelet functions, ultimately protecting mice from acute graft-versus-host disease and arterial thrombosis.[3,9,16,17] Established TRPM7 kinase substrates include annexin A1, myosin II, phospholipase C gamma 2 (PLCγ2), Ras homology family member A (RHOA), and mothers against decapentaplegic homolog 2 (SMAD2).[2,3,18–22] The phosphoinositide-3-kinase/AKT serine/threonine kinase (PI3K/AKT) and extracellular signal-related kinase (ERK1/2) signaling hubs are functionally connected,[23–25] although direct phosphorylation via TRPM7 kinase was so far not reported. TRPM7 kinase regulates differentiation of murine T lymphocytes toward proinflammatory T$_H$17 cells,[3] and AKT/mTOR-dependent neutrophil recruitment in mice.[4] TRPM7 is indispensable for lipopolysaccharide (LPS)-induced activation of murine macrophages,[6] for phagocytosis[26] and for differentiation to M1 over M2 macrophages.[27] It is thus highly involved in proinflammatory mechanisms. Concomitantly, TRPM7 promotes cell proliferation, migration, invasion, and tumor growth in human malignancies and derived cell lines, predominantly due to its ion channel capacities.[5,10,28] We recently established a link between TRPM7 kinase activity and RHOA-dependent growth of hepatocellular carcinoma,[22] yet a specific role of TRPM7 kinase over ion channel function remains understudied in the context of malignancies. The functional relation to PI3K/AKT and ERK1/2 pathways further suggests a role of TRPM7 kinase in cancerogenic signaling.

Here, we investigated a possible mechanism of TRPM7 kinase in leukemic signaling. We identified *COX-2* as proinflammatory and cancerogenic mediator downstream of TRPM7. COX-2 enhances survival and proliferation of malignant cells, while negatively influencing antitumor immunity.[29,30] We investigated the genetic ablation, genetic inactivation, or pharmacologic inhibition of TRPM7 channel-kinase in CRISPR/Cas9-edited chronic myeloid leukemia (CML)-derived HAP1 cells, and in primary CML patient cells. We observed diminished constitutive expression of *COX-2*, and reduced cell proliferation. The results pinpoint this to TRPM7 kinase directly acting on AKT as an in vitro substrate, thereby inducing *COX-2* expression downstream of AKT activation. Our data suggest a potential benefit for TRPM7 kinase inhibition in CML, chronic hematopoietic malignancies, or inflammatory conditions driven by AKT/COX-2 signaling.

Materials and Methods

Cell Culture

Wildtype (clone C631, WT) and *TRPM7*-deficient (clone 10940–04, Horizon Genomics, *KO*) HAP1 cells were reported previously.[31,32] *TRPM7-K1648R*-mutated HAP1 cells (clone HZGHK431, *KD*) were generated by CRISPR/Cas-9 genome editing at Horizon Genomics (Vienna, Austria).[22] Cells were cultured in Iscove's modified Dulbecco's medium (IMDM) containing 10% FBS. *KO* cells were supplemented with 6 mM MgCl$_2$, removed 21 h prior to experiments. Cells were grown at 37°C in a humidified atmosphere with 5% CO$_2$.

Primary Human CML Cells

Peripheral blood of patients diagnosed with CML (Table ST1) was collected by venipuncture. The study was conducted according to the guidelines of the Declaration of Helsinki, approved by the

Institutional Review Board (Ethics Committee) of the Province of Salzburg (415-E2009/2-2016, issued to RiG). PBMCs were isolated of whole blood. CD34$^+$ cells were sorted on an ARIA III (BD, USA). Cells were cultured in StemSpan SFEM II media supplemented with StemSpan CD34+Expansion Supplement and UM729 (all from Stem Cell Technologies, USA), according to the manufacturer's instructions.

Antibodies and Inhibitors

Immunoblotting: α-NFATc1 (sc-13033), α-ERK1/2 (clone C-9), α-pERK (Tyr^{204}) (sc-7383), α-pERK1/2 (Thr^{202}/Tyr^{204}) (clone D13.14.4E), α-pAKT (Thr^{308}) (clone B-5), α-NFκB p65 (cloneA-12), and α-HSP90 (clone F-8) were from Santa Cruz Biotechnology. α-LaminB1 (PA5-19468) and α-GAPDH (PA1-987) were from Thermo Fisher Scientific. α-pAKT (Ser^{473}) (clone D9E), α-AKT (clone C67E7), and α-pCREB (Ser^{133}) (clone 87G3) were from Cell Signaling Technology. α-pTRPM7 (Ser^{1511}) was described previously.[33] HRP-linked secondary antibodies were from Thermo Scientific (goat anti-rabbit) or Cell Signaling Technology (horse anti-mouse). Inhibitors TG100-115 (S1352), IPI-549 (Eganelisib, S8330), and GSK2269557 (Nemiralisib, S7937) were from SelleckChem. Thapsigargin (T9033) was from Sigma–Aldrich. NS8593 (N-196) was from Alomone. Imatinib (SML1027) was from Sigma–Aldrich.

Inductively Coupled Plasma Mass Spectrometry

HAP1 cell pellets were analyzed using inductively coupled plasma mass spectrometry (ICP-MS, ALS Scandinavia), as reported previously.[32] Briefly, cells were grown in 125 cm^2 flasks until 50%–75% confluency, trypsinized, washed, and collected by centrifugation. Cell pellets were dried at 70°C before analysis. Elementary contents of Mg or Zn were normalized to sulfur.

Electrophysiology

TRPM7 currents were acquired via whole-cell patch clamp. A ramp from -100 to $+100$ mV over 50 ms acquired at 0,5 Hz and a holding potential of 0 mV was applied. Inward and outward current amplitudes were extracted at -80, respectively, $+80$ mV. Data were normalized to cell size measured after whole-cell break in (pA/pF^{-1}). Capacitance was measured using the capacitance cancellation (EPC-10, HEKA). Mg^{2+}-free extracellular solution (in mM): 140 NaCl, 3 CaCl$_2$, 2.8 KCl, 10 HEPES-NaOH, 11 glucose (pH 7.2, 290–300 mOsm). Intracellular solution (in mM): 120 Cs-glutamate, 8 NaCl, 10 Cs-EGTA, 5 EDTA (pH 7.2, 290–300 mOsm).

Calcium Imaging

HAP1 cells were seeded into ibidi μ-dishes (Ibidi). Intracellular Ca^{2+} was monitored with Fura-2 AM (SantaCruz) using dual excitation at 340 and 380 nm, emission at 520 nm. Cells were loaded with 3 μM Fura-2 AM and 0.05% Pluronic F-127 (Invitrogen) in imaging buffer, 15 min at 37°C. Cells were washed with buffer (in mM): 140 NaCl, 2 CaCl$_2$, 4 KCl, 0.4 MgCl$_2$, and 10 HEPES-NaOH (pH 7.3). Time lapse images were acquired on an Anglerfish imager, using 5 μM thapsigargin (Thermo Fisher) to mobilize intracellular Ca^{2+}. Images were analyzed with Fiji.

Nuclear Extraction

A Nuclear Extract Kit (Active Motif, 40010) was applied according to the manufacturer's instructions.

Sodium Dodecyl Sulfate–Polyacrylamide Gel Electrophoresis and Western Blotting

Lysates were prepared in RIPA buffer and diluted with 4x Laemmli buffer (62.5 mM Tris/HCl, 20% (v/v) glycerol, 5% (v/v) β-mercaptoethanol, 4% (w/v) SDS, and 0.1% (w/v) bromophenol blue), heated to 60°C (analysis of TRPM7), respectively, 95°C (other proteins) for 5 min and separated by sodium dodecyl sulfate–polyacrylamide gel electrophoresis (SDS-PAGE). Proteins were transferred onto nitrocellulose or polyvinylidene fluoride membranes, blocked with 5% BSA or skim milk in TBST buffer. Membranes were incubated with respective antibodies according to standard procedures. Immune reactivity was quantified via densitometry (Bio-Rad). Samples were normalized to untreated and/or WT samples, and loading controls. Data were analyzed with ImageJ.

Bio-Plex Assay

For Bio-Plex Pro^{TM} Cell Signaling Assay (Bio-Rad), cells were preincubated with DMSO, NS8593 (30 μM), TG100-115 (20 μM), or IPI-549 (160 nM, Eganelisib) plus GSK2269557 (100 nM, Nemiralisib) for 30 min. Cells were lysed using Cell Signaling Reagent Kit (Bio-Rad). Samples were processed according to the manufacturer's instructions, against targets: pAKT (Ser^{473}, 171-V50001M), pERK1/2 (Thr^{202}/Tyr^{204}, Thr^{185}/Tyr^{187}, 171-V50006M), and pSMAD2 (Ser^{465}/Ser^{467}, 171-V50019M). Data were normalized to the total protein or beta-actin.

mRNA Isolation

mRNA was isolated from cell pellets, either by RNeasy Mini Kit (Qiagen) according to the instructions, or as follows: pellets were resuspended in 1 mL TRIzol (Thermo Fisher Scientific, 15596-026) and incubated for 5 min at RT. A volume of 200 μL trichloromethane/chloroform was added, samples shaken for 15 s, incubated for 3 min at RT, and centrifuged with 8000 g for 15 min at 4°C. The aqueous phase was transferred, mixed with 500 μL isopropanol and incubated for 10 min at RT. After centrifugation, supernatant (SN) was discarded and the RNA-pellet washed with 1 mL 75% ethanol. Centrifugation with 7500 rpm for 5 min at 4°C was followed by discarding the SN and drying the pellet for 30–40 min at RT. RNA samples were resuspended in 10–12 μL DEPC-treated H$_2$O, heated to 55°C for 10 min, and concentration was determined via OD measurement.

cDNA Synthesis and Quantitative Real-Time Polymerase Chain Reaction (qRT-PCR)

For cDNA synthesis, up to 4 μg mRNA was diluted in H$_2$O, mixed with 1 mM dNTP and 0.5 μg Oligo(dT)$_{12-18}$ and incubated for 5 min at 65°C. On ice, 5x First-Strand Buffer, 1 mM dithiothreitol (DTT) and DEPC-treated H$_2$O were added. After incubation at 42°C for 2 min, SuperScript II Reverse Transcriptase (Thermo Fisher Scientific) was added and incubated for 50 min at 42°C. Samples were heated to 70°C for 15 min. Transcripts were analyzed by specific primer pairs. Master mixes additionally contained cDNA diluted 1:20, and SYBR Green (Thermo Fisher

Scientific or Sigma–Aldrich). Transcripts were measured in technical triplicates on a LightCycler 480 (Roche) or a CFX-96 (Bio-Rad): 50°C 2′, 95°C 10′ (preincubation), 95°C 15″, 62°C 30″, 72°C 30″, 40 cycles (amplification), 95°C 10″, 60°C 1′ (melting), 40°C 10′ (cooling). Primer pairs: (all human, 5′–3′): *hCOX-2* (fw) TGTATGTATGAGTGTGGGATTTGAC and (rev) GATCATCTCTGC-CTGAGTATCTTTG, *hCOX-2* (fw) GAGTTATGTGTTGACATCCA-GATCAC and (rev) GCTGCTTTTTACCTTTGACACCC, *hCOX-1* (fw) CACAGTGCGCTCCAACCTTA and (rev) CTTTGGTTCCATGGGT-GTG, *hHPRT1* (fw) AAGCTTGCTGGTGAAAAGGA and (rev) AAGCAGATGGCCACAGAACT, or *hHPRT1* (fw) CCCTGGCGTCGT-GATTAGTG and (rev) TCGAGCAAGACGTTCAGTCC. *COX-2* was acquired by two distinct primer pairs on the same samples, and pooled for statistical analysis. A minimum of three independent experiments were performed. CT values of housekeeping transcripts were subtracted from measured CT values, to calculate $2^{(-\triangle CT)}$ values.

COX-2 Promoter Activity Assay

HAP1 cells were seeded into 24-well plates at equal cell numbers, and left to attach during 6 h incubation. Cells were then transfected with pDRIVE5-Lucia plasmid containing the *hCOX-2* promoter to express secreted Lucia luciferase (InvivoGen). Transfection was performed using the TransIT-X2 system (Mirus Biologicals) on Opti-MEM carrier medium (Gibco), according to instructions. If applicable, drugs were added at this point. After 22 h, 20 uL supernatant were combined with 50 uL of 1x Quanti-Luc4 reagent (InvivoGen), and product was measured on a GloMax luminescence reader (Promega), with 0.1 s reading time. At least 4 independent experiments were performed. Data were normalized to respective wildtype or DMSO control readout of the individual experiments, and compared to GFP expression of a control plasmid. Untransfected wells were measured alongside all conditions.

COX Activity Assay

HAP1 cell pellets were lysed with ice cold lysis buffer [DPBS + 1% (w/v) NP40/Igepal + protease inhibitor (Roche)]. Samples were rotated for 30 min at 4°C, centrifuged with 12 500 rpm for 5 min at 4°C, supernatant was transferred into a new reaction tube on ice. COX Activity Assay (Abcam, ab204699) was performed according to the manufacturer's instructions, in doublets. Peroxidase activity was read on a microplate reader.

In Vitro Kinase Assay

Purified recombinant human full-length inactive AKT1-GST (A16-14 G) and GST (G52-30 U) were from SignalChem. RBC HotSpot kinase assay was performed by Reaction Biology Corp. (Woolbridge, USA). Standard reaction buffer contained: 20 mM HEPES, pH 7.5, 10 mM $CaCl_2$, 1 mM EGTA, 0.01% Brij35, 0.02 mg/mL BSA, 0.1 mM Na_3VO_4, 2 mM DTT, 1% DMSO, and 2 mM $MnCl_2$. Assays were carried out with 4 μM ^{33}P-ATP, 4 μM protein substrate or GST control, and 20 μM mannose binding protein (MBP) control substrate. TRPM7 channel-kinase (Carna Biosciences, 10-111) was titrated from 50 nM in a 2-fold serial dilution. Incorporation of radioactive ^{33}P was analyzed. Raw data were converted to nM substrate phosphorylated, based on readout for 4 um ^{33}P-ATP. Kinase alone was deducted as background. In addition, data were calculated as ^{33}P incorporated per nM enzyme substrate. Reactions were carried out in duplicates, incubating for 1 h.

Fluorescence Microscopy

Localization of NFATc1 was acquired on a Zeiss LSM 780 microscope, using a 63x oil objective. Cells were stimulated with 5 μM thapsigargin for 15 min, or left unstimulated. Cells were permeabilized with 0.1% Triton X-100 for 5 min and stained for intracellular NFAT using anti-NFATc1 antibody (1:100, Santa Cruz, 7A6) in 0.2% BSA/1% normal goat serum in PBS, and secondary anti-mouse antibody AF647 (1:1000, Cell Signaling). Cells were counterstained with DAPI (0.2 μg/mL), and mounted onto glass coverslips using Antifade ROTIMount FluorCare. Zen 3.5 software was applied. Regions of interest were defined for nuclear outlines (DAPI signals). Nuclear NFATc1 was normalized to respective DAPI intensities.

Statistics

Data were plotted with GraphPad Prism 7 or higher. Statistical analysis used two-tailed unpaired *t*-test (two samples), one-way or two-way ANOVA with multiple comparisons (more samples). qRT-PCR and imaging data were analyzed with nonparametric Mann–Whitney ranks test (two samples) or multiple comparisons test with Dunnett's correction (more samples). Western blot was analyzed by Ratio-paired *t*-test.

Illustration

The schematic was finalized with CorelDRAW X8.

Results

TRPM7-deficient HAP1 Cells Show Reduced NFAT Translocation and COX-2 Expression

To study the role of TRPM7 in cellular signaling of CML cells, the human CML-derived cell line HAP1 in which TRPM7 was ablated (*TRPM7 KO*) via CRISPR/Cas9-based genome editing was utilized.[31,32] Whole-cell patch-clamp experiments confirmed functional channel inactivity in *TRPM7 KO* cells, indicated by lacking TRPM7 current density and diminished voltage-dependent ion currents (Figure 1A).[31] Using ICP-MS, we confirmed a significant reduction in total Mg^{2+} and Zn^{2+} content of *TRPM7 KO* cells compared to WT (Figure 1B and C).[31,32] As TRPM7 also conducts Ca^{2+} ions and has been implicated in Ca^{2+} signaling, we further analyzed intracellular free Ca^{2+} concentrations ($[Ca^{2+}]_i$) in TRPM7 WT and *KO* cells using Fura-2 AM-based ratiometric imaging. Basal $[Ca^{2+}]_i$ was unaltered in *TRPM7 KO* cells compared to WT (Figure 1D); however, the Ca^{2+} mobilization from intracellular stores by depletion with thapsigargin was significantly reduced in *KO* cells (Figure 1E). Collectively, these data reinforce the notion that deletion of TRPM7 protein leads to cellular deprivation of divalent cations including Mg^{2+}, Zn^{2+}, and Ca^{2+}.[32] We investigated whether lack of TRPM7 affects the nuclear expression of Ca^{2+}-dependent nuclear factor of activated T cells (NFAT) and demonstrated via Western blot that in *TRPM7 KO* cells the basal and thapsigargin-induced nuclear expression of NFATc1 was reduced (Figure 1F). Accordingly, imaging of NFATc1 nuclear translocation in response to thapsigargin showed a significant reduction in *KO* cells, compared to WT (Figure 1G). Analogously, nuclear factor "kappa-light-chain-enhancer" of activated B cells (NFκB) p65 was reduced in *TRPM7 KO* cells (Figure S1A). Analyzing the expression of inflammatory/protumorigenic genes downstream of Ca^{2+} and
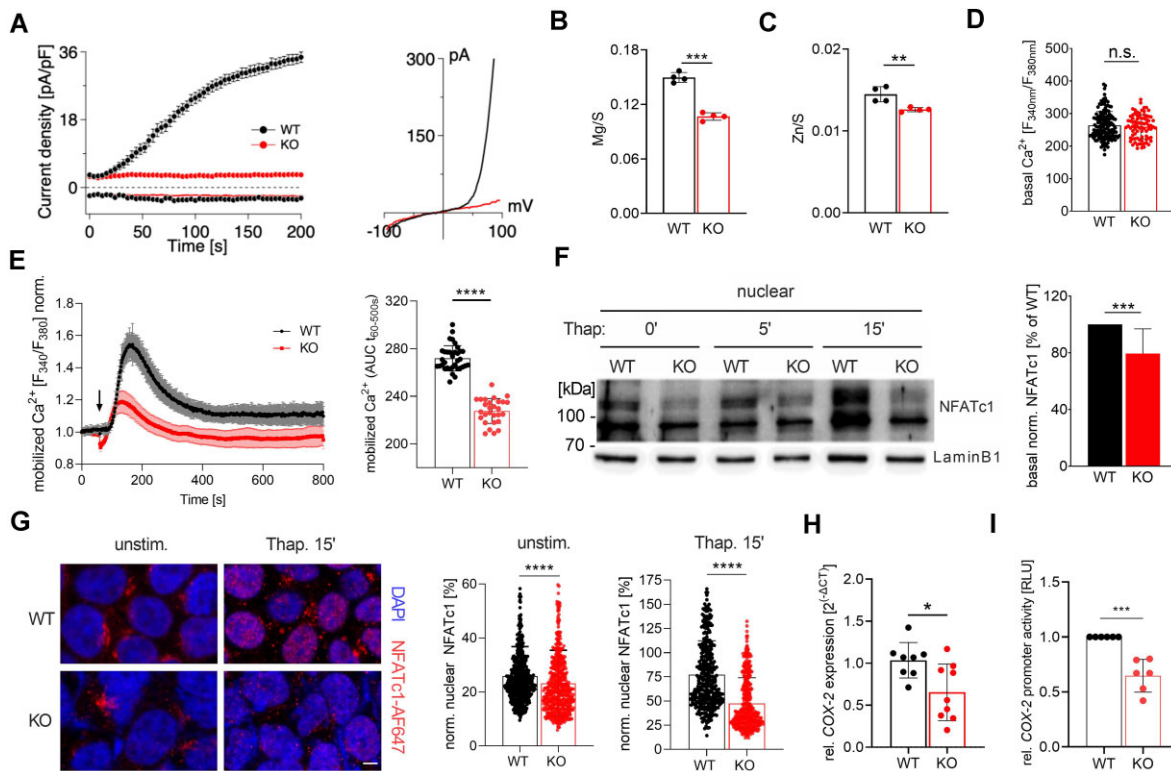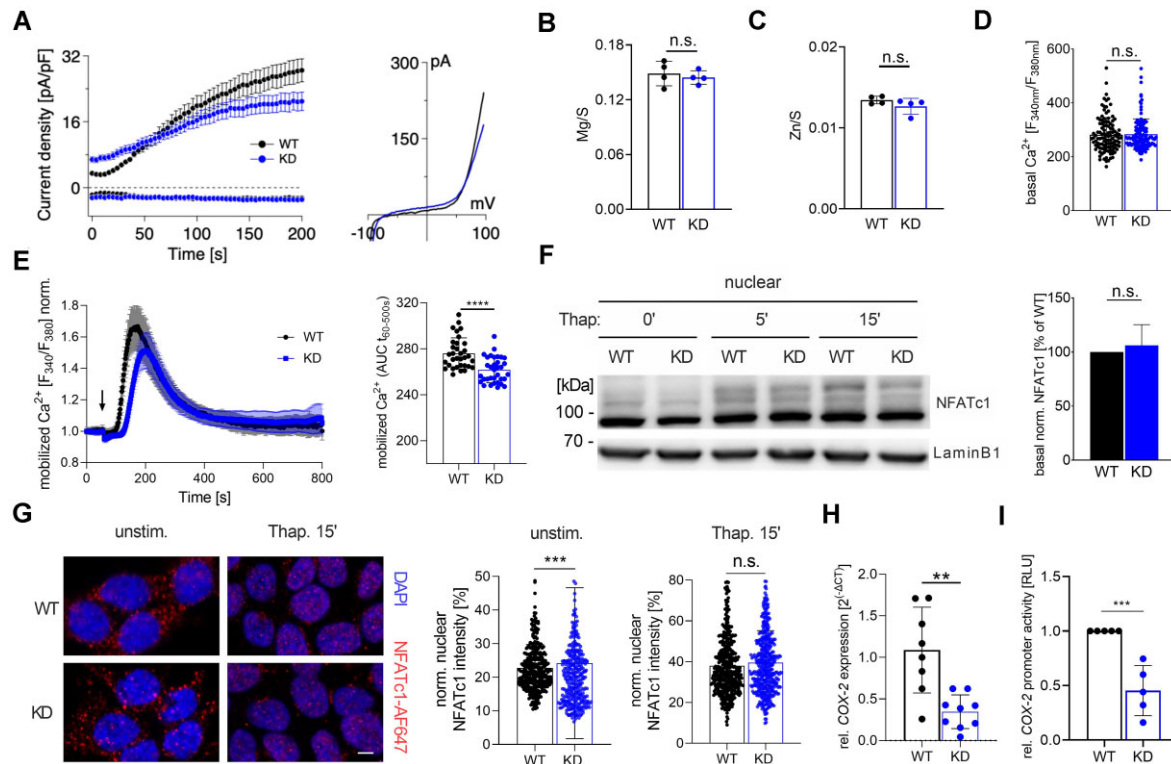
Figure 1. TRPM7 protein knockout results in reduced NFAT translocation and *COX-2* expression in HAP1 cells. (**A**) Electrophysiological characterization of TRPM7 currents in TRPM7 WT (black, $n = 11$) and *KO* (red, $n = 12$) HAP1 cells using whole-cell patch clamp. Averaged current densities at +80 and –80 mV are plotted versus time (left, mean ± SEM) and representative current–voltage (I/V) relationships extracted at 200 s are depicted (right). Note the abolished TRPM7 channel activity in *KO* cells. (**B–C**) Scatter plots of Mg^{2+} (**B**) and Zn^{2+} (**C**) ion contents in TRPM7 WT and *KO* cells assessed via ICP-MS ($n = 4$). Concentrations are counts of ion over sulfur (S), in ppm. (**D**) Fura-2 AM-based ratiometric measurements of basal Ca^{2+} concentrations in resting WT (black, $n = 149$) and *TRPM7 KO* (red, $n = 82$) HAP1 cells. (**E**) Time course (left) and quantification (right) of Fura 2-AM-based imaging of cellular Ca^{2+} mobilized from intracellular stores by stimulation with 5 μM thapsigargin (arrow). WT HAP1 cells are shown in black and *TRPM7 KO* cells in red. Right panel shows area under the curve (AUC) of stimulation response. (**F**) Western blot (left) and semiquantification (right) of nuclear NFATc1 in lysates of resting or thapsigargin-stimulated TRPM7 WT and *KO* cells. Normalized to Lamin B1 ($n = 13$). (**G**). Intracellular localization of NFATc1 in TRPM7 WT and *KO* cells, by confocal microscopy. Cells were stimulated with thapsigargin, or left unstimulated (exemplary images, left panel). Quantification gives nuclear NFATc1 stain normalized over DAPI signal (right panels, $n = 374$–555 cells). Scale bar: 5 μm. (**H**) Relative *COX-2* mRNA expression in WT (black) and *TRPM7 KO* (red) HAP1 cells, assessed by qRT-PCR. Data were related to respective housekeeping controls and depicted as $2^{-\Delta CT}$ ($n = 8$–9 triplicates). (**I**) Relative *COX-2* promoter activity in HAP1 WT or *TRPM7 KO* cells, assessed by a luminescence reporter assay on secreted Lucia luciferase ($n = 6$). Statistics: Student's *t*-test (**B, C, F, I**) or Mann–Whitney ranks test (**D, E, G, H**), $*P < .05$, $**P < .005$, $***P < .0005$, $****P < .00005$, and n.s.—not significant. Data are mean ± SD.

NFAT signaling highlighted a selective reduction in the constitutive expression of *COX-2* mRNA in *TRPM7 KO* cells (Figure 1H), while *COX-1* and *MYC* were unaltered (Figure S1B and C). *COX-2* expression upon thapsigargin stimulation increased with treatment, compared to untreated WT cells, while *KO* cells showed reduced *COX-2* throughout all conditions (Figure S1D). The lower expression of *COX-2* mRNA was reflected by significantly reduced *COX-2* promoter activity (Figure 1I) and diminished COX protein activity in *TRPM7 KO* cells (Figure S1E). Besides NFATc1, we examined the nuclear content of phosphorylated CREB, which can serve as calcium-driven signaling entity to induce *COX-2* expression.[34] Nuclear pCREB was comparable in *TRPM7 KO* and WT cells (Figure S1F). Basal nuclear expression of pCREB was generally high in HAP1 cells (Figure S1F). In conclusion, we show manifold alterations in cellular ion homeostasis and signaling in *TRPM7 KO* HAP1 cells, including reduced expression of the inflammation marker *COX-2*.

TRPM7 Kinase Regulates COX-2 Expression Independent of NFAT Activation

To understand the specific contribution of TRPM7 kinase moiety to cellular signaling and *COX-2* expression, CRISPR/Cas-9-edited

HAP1 cells with a point mutation at the TRPM7 kinase active site (TRPM7[K1648R], *kinase-dead*, *KD*)[22] were employed. Western blot of an auto-phosphorylation site of TRPM7 (pSer[1511]) confirmed the disrupted TRPM7 kinase activity (Figure S2A),[22] and patch-clamp confirmed a functional TRPM7 channel in *KD* cells (Figure 2A).[22] Using ICP-MS, we found unaltered Mg^{2+} and Zn^{2+} contents in *TRPM7 KD* cells compared to WT cells (Figure 2B and C). Analysis of basal $[Ca^{2+}]_i$ using Fura-2 AM revealed no changes in *TRPM7 KD* cells (Figure 2D). Compared to *TRPM7 KO* cells, Ca^{2+} mobilization from intracellular stores resulted in a shifted, yet less-pronounced reduction of mobilized Ca^{2+} in *TRPM7 KD* cells (Figure 2E). Our data therefore confirm a modulation of store-operated calcium entry by TRPM7 kinase, as has been described previously in other cell types.[9,35] However, nuclear expression of NFATc1 was unaffected in *TRPM7 KD* cells (Figure 2F), and nuclear NFATc1 translocation in response to thapsigargin was not altered compared to WT (Figure 2G). Importantly, we found a persistent reduction of *COX-2* mRNA expression and *COX-2* promoter activity in *TRPM7 KD* cells (Figure 2H and I), similar to our observations in *TRPM7 KO* cells. *COX-1* mRNA was unaffected (Figure S2B). Analogously to NFATc1, nuclear NFκB p65 and pCREB levels were unaltered at high levels in *TRPM7 KD* cells (Figure S2C and D). Together, by investigating *TRPM7 KD*

Figure 2. Targeted inactivation of TRPM7 kinase reduces *COX-2* expression without affecting NFAT translocation. (**A**) Electrophysiological characterization of TRPM7 currents in TRPM7 WT (black, $n = 12$) and *KD* (blue, $n = 9$) HAP1 cells using whole-cell patch clamp. Averaged current densities at +80 and –80 mV are plotted versus time (left, mean ± SEM) and representative current–voltage (*I/V*) relationships extracted at 200 s are depicted (right). (**B–C**) Scatter plots of Mg^{2+} (**B**) and Zn^{2+} (**C**) ion contents in TRPM7 WT and *KD* cells assessed via ICP-MS and analyzed as in Figure 1B ($n = 4$). (**D**) Fura-2 AM-based ratiometric measurements of basal Ca^{2+} concentrations in resting WT (black, $n = 113$) and *TRPM7 KD* (blue, $n = 199$) HAP1 cells. (**E**) Time course (left) and quantification (right) of Fura 2-AM-based imaging of Ca^{2+} mobilized from intracellular stores by stimulation with 5 μM thapsigargin (arrow). WT HAP1 cells are shown in black and *TRPM7 KD* cells in blue. Right panel shows AUC of stimulation response. (**F**) Western blot (left) and semiquantification (right) of nuclear NFATc1 in lysates of resting or thapsigargin-stimulated TRPM7 WT and *KD* cells. Normalized to Lamin B1 ($n = 10$). (**G**) NFATc1 localization in TRPM7 WT and *KD* cells, by confocal microscopy. Cells were stimulated with thapsigargin, or left unstimulated (exemplary images, left panel). Quantification gives nuclear NFATc1 stain normalized over DAPI signal (right panels, $n = 331$–359 cells). Scale bar: 5 μm. (**H**) Relative *COX-2* mRNA expression in WT (black) and *TRPM7 KD* (blue) HAP1 cells, assessed by qRT-PCR. Data were related to respective housekeeping controls and depicted as $2^{-\Delta CT}$ ($n = 8$–9 triplicates). (**I**) Relative *COX-2* promoter activity in HAP1 WT or *TRPM7 KD* cells, assessed by a luminescence reporter assay on secreted Lucia luciferase ($n = 5$). Statistics: Student's *t*-test (**B**, **C**, **F**, **I**) or Mann–Whitney ranks test (**D**, **E**, **G**, **H**), ∗∗$P < .005$, ∗∗∗$P < .0005$, ∗∗∗∗$P < .00005$, and n.s.—not significant. Data are mean ± SD.

cells with its still intact ion channel but disrupted kinase signaling domain, we identified a functional role of TRPM7 kinase in inducing *COX-2* expression, that acts separate from TRPM7 ion channel mechanisms.

TRPM7 Kinase Induces COX-2 Expression Via Phosphorylation of AKT

Typically, *COX-2* expression is regulated via NFAT, NFκB, and/or CREB transcription factors.[34,36,37] We showed that TRPM7 kinase affects *COX-2* expression independently of NFATc1, CREB, or NFκB in the HAP1 clones. SMAD2, AKT, and ERK1/2 signaling entities are also considered upstream of *COX-2* induction[38–40]— each representing reported signaling factors downstream of TRPM7 kinase.[3,24] We first analyzed phosphorylation of SMAD2 (Ser[465]/Ser[467]), a direct target of TRPM7 kinase downstream of TGF-ß, that induces inflammatory Th17 cells[3] and lung fibrosis[41] and may also be involved in TGF-ß-dependent induction of *COX-2*.[40,42,43] pSMAD2 was significantly reduced in *TRPM7 KO* and *KD* cells compared to WT HAP1 cells (Figure S3A and B), confirming previous findings. Applying the TRPM7 channel blocker NS8593 (*NS*)[44,45] to WT cells further confirmed the kinase-effect on pSMAD2, compared to controls (DMSO, and the SK-channel

blocker Apamin as off-target control for NS) (Figure S3C). Due to kinases requiring magnesium ions to function, targeting TRPM7 with NS simultaneously also blocks TRPM7 kinase mechanisms, as shown previously.[4,22] A kinase inhibitor targeting TRPM7 alongside PI3K kinase, TG100-115 (*TG*),[33,46] showed no significant effect on pSMAD2 here, similar to controls [PI3K-targeting Eganelisib (*EGA*) and Nemiralisib (*NEM*)] (Figure S3D). Since SMAD activity has also been linked to activation of AKT,[47] and PI3K/AKT signaling serves downstream of TRPM7,[23,24] we investigated AKT signaling in the HAP1 clones. As depicted in Figures 3A and S4A, *TRPM7 KO* cells showed significantly reduced phosphorylation of AKT (Ser[473]), compared to WT. By applying the TRPM7 blocker *NS* to WT cells, we confirmed the reduction of phosphorylated AKT (Ser[473]) (Figure 3B) and an accompanying reduction of *COX-2* expression (Figure 3C) and *COX-2* promoter activity (Figure S3E), compared to controls or to *COX-1* expression (Figure S3F). In line with our results on *COX-2*, in *TRPM7 KD* cells lacking TRPM7 kinase activity, we identified significantly reduced levels of pAKT (Ser[473]) (Figures 3D and S4B). This was further reflected by significantly reduced pAKT (Ser[473]) activation in response to serum stimulation, in *KD* cells (Figure S4C). Analogously, applying the TRPM7 kinase/PI3K inhibitor *TG* resulted in a significant reduction of pAKT (Ser[473])
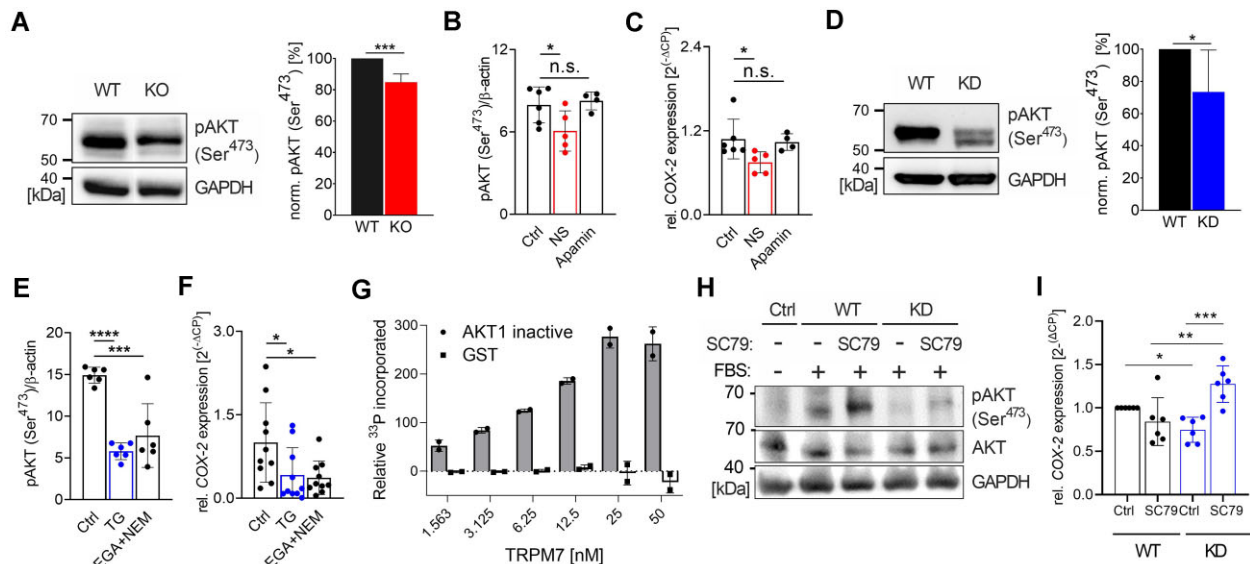
Figure 3. TRPM7 kinase induces *COX-2* expression via AKT phosphorylation. (**A**) Representative Western blot (left) and semiquantification (right) of the basal phosphorylation of AKT (Ser^{473}) in TRPM7 WT versus *KO* HAP1 lysates. Signals were normalized to respective GAPDH housekeeping controls, depicted as % of WT ($n = 8$). (**B**) pAKT (Ser^{473}) levels in pharmacologically treated HAP1 WT cells, assessed by BioPlex technology ($n = 4$–5). Cells were treated with TRPM7 channel inhibitor NS8593 (*NS*, red, 30 μM), the K$^+$ channel inhibitor Apamin as control (200 nM), or DMSO control. (**C**) Relative *COX-2* mRNA expression in inhibitor-treated HAP1 WT cells, assessed via qRT-PCR ($n = 4$–5 triplicates). (**D**) Representative Western blot (left) and semiquantification (right) of basal pAKT (Ser^{473}) in TRPM7 WT and *KD* HAP1 lysates. GAPDH was blotted as housekeeping control ($n = 10$). (**E**) pAKT (Ser^{473}) levels in HAP1 WT cells treated with TRPM7 kinase/PI3K inhibitor TG100-115 (*TG*, blue, 20 μM), PI3K inhibitors Eganelisib (*EGA*, 160 nM) + Nemiralisib (*NEM*, 100 nM), or DMSO control. BioPlex technology was used ($n = 6$). (**F**) Relative *COX-2* mRNA expression in inhibitor-treated HAP1 WT cells, assessed via qRT-PCR. Inhibitors as in C ($n = 9$–10 triplicates). (**G**) In vitro kinase activity assay of recombinant human TRPM7 protein (titrated) on recombinant inactive AKT1-GST fusion protein (gray) or GST control (white). Phosphorylation was measured after 1 h reaction and converted to relative amount of nM ^{33}P-ATP substrate incorporated. Duplicate experiment. (**H**) Pharmacologic reconstitution of AKT activation on TRPM7 *KD* cells. Representative Western blot of pAKT (Ser^{473}) in TRPM7 WT and *KD* HAP1 cells, cultured with the AKT activator SC79 or vehicle. Lysates were prepared after 21 h serum starvation followed by 1 h serum re-addition plus respective inhibitors, plotted against unstimulated control (Ctrl). GAPDH served as housekeeping control. (**I**) Pharmacologic reconstitution of *COX-2* expression in *TRPM7 KD* cells. Relative *COX-2* mRNA expression was analyzed in TRPM7 WT (black) and *KD* HAP1 cells (blue), treated with SC79 or DMSO vehicle for 2 h, respectively ($n = 5$–6). Statistics: Student's *t*-test (**A**, **D**), one-way ANOVA (**B**, **E**), Kruskal–Wallis ranks test or multiple comparison with Dunnett's correction (**C**, **F**, **I**), *$P < .05$, **$P < .005$, ***$P < .0005$, ****$P < .00005$, and n.s.—not significant. Data are mean ± SD.

(Figure S3E) and of *COX-2* expression and promoter activity in WT cells (Figures 3F and S3G), whilst also affecting *COX-1* expression (Figure S3H). Similar outcomes were observed with the PI3K-targeting controls *EGA* and *NEM*, acting upstream of AKT (Figure 3E and F). To answer the question if TRPM7 kinase may phosphorylate AKT via direct enzyme–substrate engagement, an in vitro kinase assay was performed. This approach has been successfully applied to identify SMAD2 and RHOA as TRPM7 kinase substrates in the past.[3,22] Incubating purified recombinant TRPM7 protein and inactive AKT1 as kinase substrate, in vitro, TRPM7 kinase is able to phosphorylate AKT1 in a concentration dependent manner, compared to GST control (Figures 3G and S4D). To probe this interdependency in a cellular environment, we added the AKT activator SC79[48] to TRPM7 *KD* cells. SC79 reconstituted AKT phosphorylation and TRPM7 kinase function on *COX-2* expression, compared to control (Figure 3H and I). In addition, we investigated phosphorylation of AKT at residue Thr^{308}, which is independent of serum stimulation and equally necessary for full AKT activation.[49] Analogously, we found reduced pAKT (Thr^{308}) in *KD* cells (Figure S4E) compared to WT cells. Contrarily, basal phosphorylation of ERK1/2, a master candidate in oncogenic signaling, was not affected in *TRPM7 KO* or *KD* cells compared to WT (Figure S4F and G). Together, the AKT-dependent induction of *COX-2* expression in kinase-dead HAP1 cells, and the data obtained by the in vitro kinase assay strongly suggest AKT as major player in TRPM7-mediated *COX-2* induction.

Pharmacologic Blockade of TRPM7 Inhibits COX-2 Expression and Proliferation of CML Patient Cells

To investigate whether *COX-2* expression was also targetable by pharmacologic modulation of TRPM7 in primary human CML cells, we analyzed constitutive *COX-2* mRNA expression by qRT-PCR. CML patient peripheral blood mononuclear cells (PBMCs) were treated with the TRPM7 channel inhibitor *NS*, the TRPM7 kinase/PI3K inhibitor *TG*, or the PI3K inhibitors *EGA* + *NEM* as controls for *TG*. Preincubation of patient PBMCs with the TRPM7-inhibitors *NS* and *TG* resulted in significant reduction of constitutive *COX-2* expression, while *EGA* + *NEM* reduced *COX-2* non-significantly (Figure 4A). In line with the data obtained in the HAP1 cells, the TRPM7 inhibitors *NS* and *TG* resulted in a significant reduction of pAKT (Ser^{473}) in CML patient PBMCs, confirmed by the PI3K-inhibitors *EGA* + *NEM* (Figure 4B). SMAD2 and ERK1/2 phosphorylation were again not significantly reduced with addition of *NS*, *TG*, or controls (Figure S5A and B). To investigate the effect of TRPM7 inhibition on CML cell proliferation, we examined proliferative cell counts of sorted CD34$^+$ patient cells treated with *NS*, the CML drug Imatinib (*IMA*) targeting the oncogenic BCR::ABL kinase, or a combination of *NS* + *IMA*. An increase in dead cells, and a significant reduction of cell growth with addition of both *NS* or *IMA* was observed (Figure 4C and D). Combined treatment of cells with *NS* + *IMA* gave a combinatorial/additive effect on blocking CML cell proliferation (Figure 4C and D), suggesting that they act on distinct cellular pathways. HAP1 cells were already resistant to Imatinib (Figure S5C), but
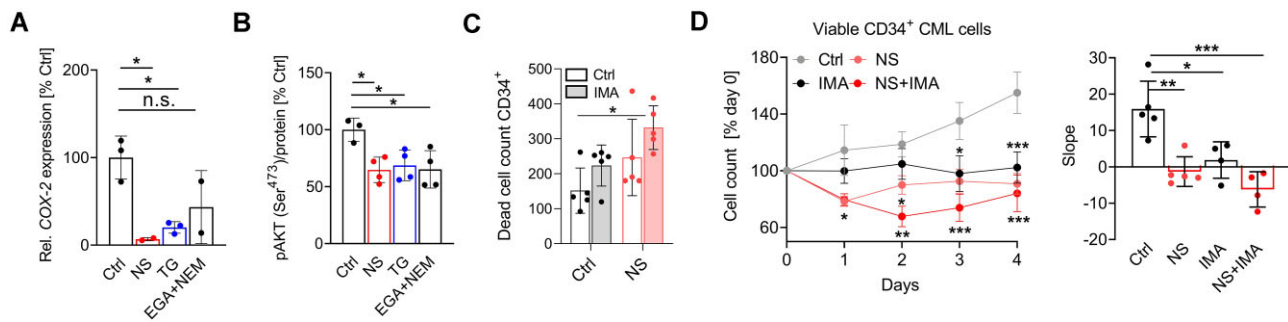
Figure 4. TRPM7 blockade decreases COX-2 expression and proliferation of primary human CML cells. (**A**) Relative expression of COX-2 mRNA in CML patient-derived PBMCs cultured in the presence of inhibitors, analyzed via qRT-PCR. Inhibitors were compared to DMSO control: TRPM7 channel inhibitor NS8593 (NS, red, 30 μM), TRPM7 kinase/PI3K inhibitor TG100-115 (TG, blue, 20 μM), PI3K inhibitors Eganelisib (EGA, 160 nM) + Nemiralisib (NEM, 100 nM). (**B**) Basal pAKT (Ser^{473}) levels in CML patient-derived PBMCs, assessed via BioPlex technology. Inhibitors as in **A** (n = 4–5). (**C–D**) Proliferation experiment of patient-derived CD34$^+$ CML cells cultured in presence of indicated inhibitors (concentrations as in **A**). Imatinib was used at 1 μM. Cells were stained with ViaCount live/dead marker. For **C**, dead cell count was plotted after 3 d incubation. For **D**, live cell counts were plotted for each indicated day, normalized to respective day 0 (left, mean ± SEM). Cell proliferation was calculated as slope of respective data curves, and compared to DMSO control (**D**, right, n = 3–5). Statistics: one-way ANOVA (**B**, **D**), two-way ANOVA (**C**), or multiple comparisons test with Dunnett's correction (**A**), $* P < 0.05$, $** P < 0.005$, $*** P < 0.005$, and n.s.—not significant. Data are mean ± SD.

were sensitized by the addition of NS, as shown by significant reduction of cell viability upon treatment (Figure S5D). Taken together, our results identify TRPM7 as a proinflammatory regulator of COX-2, particularly affecting constitutive COX-2 expression via modulating AKT signaling, in primary CML cells and CRISPR/Cas9-engineered CML-derived HAP1 clones. We observe combinatorial effects on CD34$^+$ CML cell proliferation via TRPM7 blockade together with Imatinib, a first-line candidate in the current CML treatment regimen. Thus, TRPM7 channel-kinase may provide a promising perspective as an alternative target in COX-2-driven malignant disease, that acts via BCR::ABL independent pathways.

Discussion

COX-2 has been studied extensively as a driver of inflammation and co-determinant of malignant progression. Its role as an anti-inflammatory target in clinical practice is undoubted. Chronic inflammation can drive the development and progression of cancer.[50,51] In humans, both COX isoforms contribute to inflammatory mechanisms.[52] The expression of COX-2, but not COX-1, is elevated in cancer entities including CML.[29,53,54] COX-2 enhances survival and proliferation of malignant cells, while negatively influencing antitumor immunity.[29,30] COX-2 was found significantly increased in CML patient cells compared to healthy controls, correlating with shorter survival.[29] Leukemia cells potentially produce COX-2-dependent factors that enhance angiogenesis and inflammation, correlating with poor prognosis.[30] Studies in humans indicate that therapy with COX-2 inhibitors might provide an effective approach to cancer treatment.[25,53,54] Conventional nonsteroidal anti-inflammatory drugs (NSAIDs), which inhibit COX-1 and COX-2 are commonly used to treat acute inflammation and proinflammatory diseases.[55] However, organ specific adverse effects may occur for more specific COX-2 inhibitors.[56,57] Alternate approaches for the functional inhibition of COX-2 are desirable, and cellular mechanisms that modulate COX-2 expression, inflammation, and malignancy are widely relevant. A beneficial effect of COX-2-directed add-on therapy in combination with first-line chemotherapy remains a promising scenario in cancer management.[58]

TRPM7 is an essential player in immunity and inflammation, regulating differentiation of proinflammatory lymphocytes and macrophages. It also serves as modulator in development of new malignancies, facilitating cell growth, migration, and invasion.[2,10] Takahashi et al. reported a connection between TRPM7-mediated Ca^{2+} entry and growth of the CML-derived cell line K562.[28] We confirmed this in primary CML patient cells using the TRPM7 inhibitor NS8593, with a beneficial in vitro outcome on cell proliferation, when combined with CML-directed BCR::ABL kinase inhibitor Imatinib. The targeting of distinct signaling pathways may provide an advantage in combinatorial or alternative approaches to BCR::ABL inhibitors. The latter are prone to resistance mutations, posing a significant challenge to CML therapy[59]. Our data on the Imatinib-resistant HAP1 cells support these hypotheses. We further show that inhibition of TRPM7 channel-kinase in CML and HAP1 cells results in reduction of constitutive COX-2 expression, with an insignificant effect on COX-1. Previously, TRPM7 has been suggested to induce proinflammatory mediators, including COX-2, in bradykinin-stimulated vascular smooth muscle cells as well as in aldosterone-stimulated HEK-293 cells.[60,61] By employing CRISPR/Cas9-edited TRPM7-deficient and kinase-mutated HAP1 cells, we were able to link COX-2 gene expression to TRPM7 kinase-mediated activation of AKT signaling. In murine and human neutrophils, we recently showed that TRPM7 kinase facilitates neutrophil chemotaxis and proinflammatory signatures, by inducing AKT phosphorylation.[4] Here, we show that TRPM7 kinase drives cellular signaling in CML cells, via AKT and COX-2. This is independent of TRPM7 ion channel-mediated Ca^{2+} flux or NFATc1 translocation. We show that TRPM7 kinase can phosphorylate AKT in vitro, via direct phosphorylation. In comparison, we previously found a similar activity range against RHOA protein substrate, using the same assay.[22] This is the first report of enzymatic activity of TRPM7 kinase on AKT protein, providing evidence for a potential point of action in the PI3K/AKT signaling pathway directly at the level of AKT.[4,23,24] The phosphorylated residue(s) within AKT are yet to be confirmed, and our findings do not rule out additional interactions with PI3K, or other phosphoinositide phosphate-dependent mechanisms in cells. In 2008, Sahni et al. reported a growth arrest of TRPM7-deficient lymphocytes that is rescued by expression of constitutively active PI3K subunit p100.[23] Our data indicate an enzymatic interaction of TRPM7 kinase with AKT, downstream of PI3K. For further proof of individual phospho-sites targeted within AKT, one would require follow-up experiments on purified TRPM7 and AKT proteins. While Western blot could give a first glimpse on the residues phosphorylated by TRPM7

kinase, one could also mutate the various phospho-sites of interest. Our Western blot data on cell lysates suggest that TRPM7 kinase affects both phospho-residues required for full AKT activation, that is, Ser[473] and Thr[308].[62] This could position TRPM7 as unique AKT-activating kinase. In the context of leukemia, phosphorylation of AKT (Thr[308]) has been shown to correlate with high-risk AML,[63] and a pronounced phosphorylation at Thr[308] correlates with high AKT activity in human nonsmall cell lung cancer.[64] Thus, via AKT signaling, TRPM7 kinase is functionally connected with expression of cancer-promoting genes. We have not ascertained if phosphorylation of the transcription factor SMAD2 may additionally mediate TRPM7 kinase-dependent induction of AKT/COX-2 further downstream.[3,47]

We show a potential benefit of TRPM7 blockade in enhancing CML drug sensitivity effects. A combinatorial effect with Imatinib therapy has been suggested for COX-2 inhibition.[58] Beyond its role in CML signaling, inhibition of TRPM7 channel-kinase may positively affect anti-inflammatory signals in a range of pathophysiological conditions, as may be suggested for T-cell- and neutrophil-driven chronic inflammation.[3,4] Also, TRPM7 kinase-mutated mice show protection from ischemic stroke,[3,16] hence, its pharmacologic blockade may positively affect cardiovascular risks and cancer-associated thrombotic risk. It will be relevant to dissect further roles of TRPM7 in related tissues.

Acknowledgments

Author Contributions

B.H., W.N., and S.Z. wrote the manuscript. B.H., W.N. and S.H. performed main experiments. K.H., M.F., N.Z., A.M., V.S., L.F., and L.A. performed additional experiments. D.S., V.C., Ro.G., Ri.G., A.B., I.B., and T.G. provided valuable expertise and feedback. S.Z. conceived and supervised the study. All authors revised the manuscript and agreed on publishing.

Supplementary Material

Supplementary material is available at the *APS Function* online.
    Table T1. Information on CML patients.
    Figure S1. Additional data corresponding to Figure 1.
    Figure S2. Additional data corresponding to Figure 2.
    Figure S3. Additional plots corresponding to Figure 3.
    Figure S4. Additional Western blots and assays corresponding to Figure 3.
    Figure S5. Additional data corresponding to Figure 4.

Funding

Conflict of Interest

The authors declare no conflict of financial interests. S.Z. holds the position of Editorial Board Member for *FUNCTION* and is blinded from reviewing or making decisions for the manuscript.

Data Availability

Data and materials may be requested by the corresponding author.

References

1. Zierler S, Hampe S, Nadolni W. TRPM channels as potential therapeutic targets against pro-inflammatory diseases. *Cell Calcium*. 2017;**67**:105–115.
2. Nadolni W, Zierler S. The channel-kinase TRPM7 as novel regulator of immune system homeostasis. *Cells*. 2018;**7**(8):109.
3. Romagnani A, Vettore V, Rezzonico-Jost T, et al. TRPM7 kinase activity is essential for T cell colonization and alloreactivity in the gut. *Nat Commun*. 2017;**8**(1):1917.
4. Nadolni W, Immler R, Hoelting K, et al. TRPM7 kinase is essential for neutrophil recruitment and function via regulation of Akt/mTOR signaling. *Front Immunol*. 2020;**11**: 606893.
5. Meng S, Alanazi R, Ji D, et al. Role of TRPM7 kinase in cancer. *Cell Calcium*. 2021;**96**:102400.
6. Schappe MS, Szteyn K, Stremska ME, et al. Chanzyme TRPM7 mediates the Ca^{2+} influx essential for lipopolysaccharide-induced toll-like receptor 4 endocytosis and macrophage activation. *Immunity*. 2018;**48**(1):59–74.e5.
7. Chen WL, Barszczyk A, Turlova E, et al. Inhibition of TRPM7 by carvacrol suppresses glioblastoma cell proliferation, migration and invasion. *Oncotarget*. 2015;**6**(18):16321–16340.
8. Huang L, Ng NM, Chen M, et al. Inhibition of TRPM7 channels reduces degranulation and release of cytokines in rat bone marrow-derived mast cells. *Int J Mol Sci*. 2014;**15**(7):11817–11831.
9. Beesetty P, Wieczerzak KB, Gibson JN, et al. Inactivation of TRPM7 kinase in mice results in enlarged spleens, reduced T-cell proliferation and diminished store-operated calcium entry. *Sci Rep*. 2018;**8**(1):3023.
10. Yee NS. Role of TRPM7 in cancer: potential as molecular biomarker and therapeutic target. *Pharmaceuticals*. 2017;**10**(2):39.
11. Middelbeek J, Kuipers AJ, Henneman L, et al. TRPM7 is required for breast tumor cell metastasis. *Cancer Res*. 2012;**72**(16):4250–4261.
12. Nadler MJ, Hermosura MC, Inabe K, et al. LTRPC7 is a Mg.ATP-regulated divalent cation channel required for cell viability. *Nature*. 2001;**411**(6837):590–595.
13. Ryazanova LV, Dorovkov MV, Ansari A, Ryazanov AG. Characterization of the protein kinase activity of TRPM7/ChaK1, a protein kinase fused to the transient receptor potential ion channel. *J Biol Chem*. 2004;**279**(5):3708–3716.
14. Schmitz C, Perraud AL, CO J, et al. Regulation of vertebrate cellular Mg^{2+} homeostasis by TRPM7. *Cell*. 2003;**114**(2):191–200.
15. Jin J, Desai BN, Navarro B, Donovan A, Andrews NC, Clapham DE. Deletion of Trpm7 disrupts embryonic development and thymopoiesis without altering Mg^{2+} homeostasis. *Science*. 2008;**322**(5902):756–760.
16. Gotru SK, Chen W, Kraft P, et al. TRPM7 Kinase controls calcium responses in arterial thrombosis and stroke in mice. *ATVB*. 2018;**38**(2):344–352.
17. Khajavi N, Beck A, Ricku K, et al. TRPM7 kinase is required for insulin production and compensatory islet responses during obesity. *JCI Insight*. 2023;**8**(3):e163397.

18. Runnels LW, Yue L, Clapham DE. TRP-PLIK, a bifunctional protein with kinase and ion channel activities. *Science*. 2001;**291**(5506):1043–1047.

19. Deason-Towne F, Perraud AL, Schmitz C. Identification of Ser/Thr phosphorylation sites in the C2-domain of phospholipase C gamma2 (PLCgamma2) using TRPM7-kinase. *Cell Signal*. 2012;**24**(11):2070–2075.

20. Clark K, Langeslag M, van Leeuwen B, et al. TRPM7, a novel regulator of actomyosin contractility and cell adhesion. *EMBO J*. 2006;**25**(2):290–301.

21. Dorovkov MV, Ryazanov AG. Phosphorylation of annexin I by TRPM7 channel-kinase. *J Biol Chem*. 2004;**279**(49):50643–50646.

22. Voringer S, Schreyer L, Nadolni W, et al. Inhibition of TRPM7 blocks MRTF/SRF-dependent transcriptional and tumorigenic activity. *Oncogene*. 2020;**39**(11):2328–2344.

23. Sahni J, Scharenberg AM. TRPM7 ion channels are required for sustained phosphoinositide 3-kinase signaling in lymphocytes. *Cell Metab*. 2008;**8**(1):84–93.

24. Fang L, Zhan S, Huang C, et al. TRPM7 channel regulates PDGF-BB-induced proliferation of hepatic stellate cells via PI3K and ERK pathways. *Toxicol Appl Pharmacol*. 2013;**272**(3):713–725.

25. Lu Y, Liu LL, Liu SS, et al. Celecoxib suppresses autophagy and enhances cytotoxicity of imatinib in imatinib-resistant chronic myeloid leukemia cells. *J Transl Med*. 2016;**14**:(1):270.

26. Schappe MS, Stremska ME, Busey GW, et al. Efferocytosis requires periphagosomal Ca^{2+}-signaling and TRPM7-mediated electrical activity. *Nat Commun*. 2022;**13**(1):3230.

27. Schilling T, Miralles F, Eder C. TRPM7 regulates proliferation and polarisation of macrophages. *J Cell Sci*. 2014;**127**(Pt 21):4561–4566.

28. Takahashi K, Umebayashi C, Numata T, et al. TRPM7-mediated spontaneous Ca^{2+} entry regulates the proliferation and differentiation of human leukemia cell line K562. *Physiol Rep*. 2018;**6**(14):e13796.

29. Giles FJ, Kantarjian HM, Bekele BN, et al. Bone marrow cyclooxygenase-2 levels are elevated in chronic-phase chronic myeloid leukaemia and are associated with reduced survival. *Br J Haematol*. 2002;**119**(1):38–45.

30. Bernard MP, Bancos S, Sime PJ, Phipps RP. Targeting cyclooxygenase-2 in hematological malignancies: rationale and promise. *CPD*. 2008;**14**(21):2051–2060.

31. Chubanov V, Ferioli S, Wisnowsky A, et al. Epithelial magnesium transport by TRPM6 is essential for prenatal development and adult survival. *eLife*. 2016;**5**:e20914.

32. Mittermeier L, Demirkhanyan L, Stadlbauer B, et al. TRPM7 is the central gatekeeper of intestinal mineral absorption essential for postnatal survival. *Proc Natl Acad Sci USA*. 2019;**116**(10):4706–4715.

33. Kollewe A, Chubanov V, Tseung FT, et al. The molecular appearance of native TRPM7 channel complexes identified by high-resolution proteomics. *eLife*. 2021;**10**:e68544.

34. Ghosh R, Garcia GE, Crosby K, et al. Regulation of Cox-2 by cyclic AMP response element binding protein in prostate cancer: potential role for nexrutine. *Neoplasia*. 2007;**9**(11):893–899.

35. Faouzi M, Kilch T, Horgen FD, Fleig A, Penner R. The TRPM7 channel kinase regulates store-operated calcium entry. *J Physiol*. 2017;**595**(10):3165–3180.

36. Iniguez MA, Martinez-Martinez S, Punzon C, Redondo JM, Fresno M. An essential role of the nuclear factor of activated T cells in the regulation of the expression of the cyclooxygenase-2 gene in human T lymphocytes. *J Biol Chem*. 2000;**275**(31):23627–23635.

37. Kirkby NS, Chan MV, Zaiss AK, et al. Systematic study of constitutive cyclooxygenase-2 expression: role of NF-kappaB and NFAT transcriptional pathways. *Proc Natl Acad Sci USA*. 2016;**113**(2):434–439.

38. Subbaramaiah K, Chung WJ, Dannenberg AJ. Ceramide regulates the transcription of cyclooxygenase-2. Evidence for involvement of extracellular signal-regulated kinase/c-Jun N-terminal kinase and p38 mitogen-activated protein kinase pathways. *J Biol Chem*. 1998;**273**(49):32943–32949.

39. St-Germain ME, Gagnon V, Mathieu I, Parent S, Asselin E. Akt regulates COX-2 mRNA and protein expression in mutated-PTEN human endometrial cancer cells. *Int J Oncol*. 2004;**24**(5):1311–1324.

40. Fang L, Chang HM, Cheng JC, Leung PC, Sun YP. TGF-beta1 induces COX-2 expression and PGE2 production in human granulosa cells through Smad signaling pathways. *J Clin Endocrinol Metab*. 2014;**99**(7):E1217–E1226.

41. Zeitlmayr S, Zierler S, Staab-Weijnitz CA, et al. TRPM7 restrains plasmin activity and promotes transforming growth factor-beta1 signaling in primary human lung fibroblasts. *Arch Toxicol*. 2022;**96**(10):2767–2783.

42. Ren R, Charles PC, Zhang C, Wu Y, Wang H, Patterson C. Gene expression profiles identify a role for cyclooxygenase 2-dependent prostanoid generation in BMP6-induced angiogenic responses. *Blood*. 2007;**109**(7):2847–2853.

43. Shao J, Sheng H, Inoue H, Morrow JD, DuBois RN. Regulation of constitutive cyclooxygenase-2 expression in colon carcinoma cells. *J Biol Chem*. 2000;**275**(43):33951–33956.

44. Chubanov V, Mederos y Schnitzler M, Meissner M, et al. Natural and synthetic modulators of SK ($K_{ca}2$) potassium channels inhibit magnesium-dependent activity of the kinase-coupled cation channel TRPM7. *Br J Pharmacol*. 2012;**166**(4):1357–1376.

45. Nadezhdin KD, Correia L, Narangoda C, et al. Structural mechanisms of TRPM7 activation and inhibition. *Nat Commun*. 2023;**14**(1):2639.

46. Song C, Bae Y, Jun J, et al. Identification of TG100-115 as a new and potent TRPM7 kinase inhibitor, which suppresses breast cancer cell migration and invasion. *Biochim Biophys Gen Sub*. 2017;**1861**(4):947–957.

47. Xiong S, Cheng JC, Klausen C, Zhao J, Leung PC. TGF-beta1 stimulates migration of type II endometrial cancer cells by down-regulating PTEN via activation of SMAD and ERK1/2 signaling pathways. *Oncotarget*. 2016;**7**(38):61262–61272.

48. Jo H, Mondal S, Tan D, et al. Small molecule-induced cytosolic activation of protein kinase Akt rescues ischemia-elicited neuronal death. *Proc Natl Acad Sci USA*. 2012;**109**(26):10581–10586.

49. Scheid MP, Woodgett JR. Unravelling the activation mechanisms of protein kinase B/Akt. *FEBS Lett*. 2003;**546**(1):108–112.

50. Huber S, Gagliani N, Zenewicz LA, et al. IL-22BP is regulated by the inflammasome and modulates tumorigenesis in the intestine. *Nature*. 2012;**491**(7423):259–263.

51. Gagliani N, Hu B, Huber S, Elinav E, Flavell RA. The fire within: microbes inflame tumors. *Cell*. 2014;**157**(4):776–783.

52. Smith WL, Garavito RM, DeWitt DL. Prostaglandin endoperoxide H synthases (cyclooxygenases)-1 and -2. *J Biol Chem*. 1996;**271**(52):33157–33160.

53. Dannenberg AJ, Altorki NK, Boyle JO, et al. Cyclo-oxygenase 2: a pharmacological target for the prevention of cancer. *Lancet Oncol.* 2001;**2**(9):544–551.

54. Hashemi Goradel N, Najafi M, Salehi E, Farhood B, Mortezaee K. Cyclooxygenase-2 in cancer: a review. *J Cell Physiol.* 2019;**234**(5):5683–5699.

55. Rainsford KD. Anti-inflammatory drugs in the 21st century. *Subcell Biochem.* 2007;**42**:3–27.

56. Bertagnolli MM. Chemoprevention of colorectal cancer with cyclooxygenase-2 inhibitors: two steps forward, one step back. *Lancet Oncol.* 2007;**8**(5):439–443.

57. Li P, Zheng Y, Chen X. Drugs for autoimmune inflammatory diseases: from small molecule compounds to anti-TNF biologics. *Front Pharmacol.* 2017;**8**:460.

58. Li S, Jiang M, Wang L, Yu S. Combined chemotherapy with cyclooxygenase-2 (COX-2) inhibitors in treating human cancers: recent advancement. *Biomed Pharmacother.* 2020;**129**:110389.

59. Massimino M, Stella S, Tirro E, et al. ABL1-directed inhibitors for CML: efficacy, resistance and future perspectives. *Anticancer Res.* 2020;**40**(5):2457–2465.

60. Yogi A, Callera GE, O'Connor S, et al. Aldosterone signaling through transient receptor potential melastatin 7 cation channel (TRPM7) and its alpha-kinase domain. *Cell Signalling.* 2013;**25**(11):2163–2175.

61. Yogi A, Callera GE, Tostes R, Touyz RM. Bradykinin regulates calpain and proinflammatory signaling through TRPM7-sensitive pathways in vascular smooth muscle cells. *Am J Physiol-Regul, Integr Comp Physiol.* 2009;**296**(2):R201–R207.

62. Alessi DR, James SR, Downes CP, et al. Characterization of a 3-phosphoinositide-dependent protein kinase which phosphorylates and activates protein kinase Balpha. *Curr Biol.* 1997;**7**(4):261–269.

63. Gallay N, Dos Santos C, Cuzin L, et al. The level of AKT phosphorylation on threonine 308 but not on serine 473 is associated with high-risk cytogenetics and predicts poor overall survival in acute myeloid leukaemia. *Leukemia.* 2009;**23**(6):1029–1038.

64. Vincent EE, Elder DJ, Thomas EC, et al. Akt phosphorylation on Thr308 but not on Ser473 correlates with Akt protein kinase activity in human non-small cell lung cancer. *Br J Cancer.* 2011;**104**(11):1755–1761.